Theoretical and Experimental Chemistry, Vol. 48, No. 5, November, 2012 (Russian Original Vol. 48, No. 5, September-October, 2012)

MORPHOLOGY, PHOTOCHEMICAL AND PHOTOCATALYTIC PROPERTIES OF NANOCRYSTALLINE ZINC OXIDE FILMS

A. V. Kozytskiy,[1] A. L. Stroyuk,[1] S. Ya. Kuchmy,[1] N. A. Skorik,[2] and V. O. Moskalyuk[2]

UDC 544.174.2,544.77.051

Electrodeposition was used to obtain ZnO films on indium tin oxide (ITO) consisting of microplates with diameter 0.5-2.0 μm and thickness 50-300 nm, which, in turn, consist of two particle fractions: relatively large particles with diameter 20-40 nm and fine particles with diameter of about 5 nm. It was found that the fine particles permit these ZnO films to undergo photoinduced charging. This property of ZnO films markedly affects the kinetics of the photocatalytic reduction of $NaAuCl_4$ by ethanol.

Key words: *electrodeposition, ZnO films, Burstein–Moss effect, photocatalysis, gold nanoparticles.*

The electrodeposition of zinc oxide on the surface of conducting plates such as indium tin oxide (ITO) and fluoro-doped tin oxide (FTO) is a relatively available and efficient method for the preparation of nanostructural ZnO films with readily adjustable thickness and morphology [1-3]. In light of these advantages, electrodeposition is being used ever more commonly for the preparation of nanocrystalline ITO/ZnO films as components of solar cell photoanodes [1-4]. Quantum-sized effects characteristic for ZnO particles with diameter less than 10 nm and also their capacity to undergo photoinduced charging, which has been studied adequately for ZnO colloids [5-8], has stimulated interest in such films as an alternative to photoanodes derived from nanocrystalline TiO_2. Furthermore, analysis of publications on the electrodeposition of ZnO films has shown that the photochemical properties of such materials, especially, aspects of photoinduced charging of the films and its effect on photocatalytic surface reactions, have hardly been investigated.

Hence, we studied the structural and spectral properties of electrodeposited ZnO films, established the feasibility of photoinduced charging of these films upon the action of continuous irradiation with near-UV light, and elucidated various features of the photocatalytic reduction of $NaAuCl_4$ by ethanol on the surface of ZnO films. The basis for this study was our previous data on the strong effect of the photocharging of colloidal ZnO/Au nanoparticles on the dynamics of this photocatalytic reaction [7].

EXPERIMENTAL

We used $Zn(NO_3)_2$, KCl, $NaAuCl_4$, metallic zinc, polyvinylpyrrolidone (PVP, molecular mass M_w = 360,000 g/mol) and glass plates with a deposited conducting layer of mixed indium tin oxide (ITO) with specific resistance 70 Ω/cm^2 supplied

[1]L. V. Pisarzhevskii Institute of Physical Chemistry, National Academy of Sciences of Ukraine, Prospekt Nauky, 31, Kyiv 03028, Ukraine. E-mail: stroyuk@inphyschem-nas.kiev.ua.
[2]NanoMedTech, Vul. Gor'kogo, 68, Kyiv 03150, Ukraine.

Translated from Teoreticheskaya i Éksperimental'naya Khimiya, Vol. 48, No. 5, pp. 308-314, September-October, 2012. Original article submitted October 9, 2012.

by Sigma Aldrich. In order to remove water, a sample of 96 vol.% ethanol was heated prior to use over roasted calcium oxide and then distilled, taking the middle fraction.

Nanocrystalline zinc oxide films on the surface of ITO plates were prepared by electrodeposition using a three-electrode scheme by analogy with the method described by Chen [2]. The working electrode was a 5×30-mm ITO plate. The counter electrode was composed of zinc foil. A silver chloride reference electrode was used. The deposition was carried out over 10 min at –1.3 V vs. Ag/AgCl and 60 °C. The electrolyte containing 50 vol.% ethanol, 50 vol.% distilled water, 0.1 mol/L $Zn(NO_3)_2$, 0.1 mol/L KCl, and 4.0 g/L PVP was stirred with a magnetic stirrer. The potentials were applied using a Keithley 2400 multimeter. Prior to electrodeposition, the zinc electrode was activated by maintenance for 1-2 min in 0.1 mol/L hydrochloric acid. After electrodeposition, the films were washed with distilled water and 2-propanol, dried at 70 °C, and roasted in the air at 400 °C.

The photochemical experiments were carried out in sealed glass ampoules, from which dissolved air was removed prior to irradiation by bubbling argon. The samples were irradiated by filtered light from a 1000-W high-pressure mercury lamp in the range λ = 310-390 nm with integral intensity 25 mW/cm^2.

The absorption spectra of the films or ampoules with immersed films were taken on a Specord 210 spectrophotometer relative to ITO. Scanning electron microphotographs (SEM) of the films were obtained using a Mira3 Tescan microscope with accelerating voltage 5-20 kV. The X-ray phase analysis (XPA) was carried out on a Bruker D8 Advance diffractometer using copper K_α radiation (λ = 0.154 nm).

RESULTS AND DISCUSSION

Electrolysis of water–ethanol mixtures containing $Zn(NO_3)_2$, KCl, and PVP leads to the formation of a light-scattering layer on the ITO surface, which, according to the scanning electron microscopy (SEM) data, consists of individual plates with longitudinal dimension reaching 2 μm and thickness 50-300 nm (Fig. 1a,b). The diffraction patters of the films in Fig. 1c, curve 1 display a set of reflections characteristic for zinc hydroxochloride $Zn_5(OH)_8Cl_2{\cdot}2H_2O$ as well as reflections belonging to ITO (Fig. 1c, insert). The formation of this compound is characteristic for systems containing zinc nitrate and, according to literature data [1-3, 9], proceeds by the following scheme: (on the cathode) $NO_3^- + H_2O + 2e^- \rightarrow NO_2^- + 2OH^-$, $5Zn^{2+} + 8OH^- + 2Cl^- \rightarrow Zn_5(OH)_8Cl_2$; (on the anode) $Zn^0 \rightarrow Zn^{2+} + 2e^-$.

Figure 1 shows that the reflections in the diffraction pattern of zinc hydroxochloride corresponding to the planes [003], [006], and [0012] oriented perpendicular to the *Z* axis are the most pronounced. The finding of a strong reflection at 2θ = 11° indicates a laminar structure of the particles of electrodeposited $Zn_5(OH)_8Cl_2{\cdot}2H_2O$ with interplane distance on the order of 8 Å [10-12].

Roasting the zinc hydroxochloride films on ITO does not lead to discernible change in the morphology of the films as a whole but markedly affects the structure of the component microplates. Figure 1 shows that the microplates, which are smooth and homogeneous on the surface prior to roasting (Fig. 1b), become granular and porous after heat treatment at 400 °C (Fig. 1d). The diameter of the individual granules in the microplates is 20-40 nm. The film thickness determined using SEM data from chips cleaved off the films is 2.5 μm.

The diffraction pattern of the roasted films given in Fig. 1c, curve 2 displays a set of several broadened reflections characteristic for hexagonal zinc oxide. The diameter of the individual crystallites calculated from the spectral width of the [002] reflection using the Scherrer equation [3] is 20 nm, which is in accord with the SEM data. Hence, roasting of the ITO/$Zn_5(OH)_8Cl_2$ films leads to the conversion of zinc hydroxochloride into zinc oxide on the ITO film surface, which may be described by the chemical equation $Zn_5(OH)_8Cl_2 \rightarrow 5ZnO + 2HCl + 3H_2O$. The shape of the ZnO microplates comprising the film (Fig. 1d) is given by the planar shape of the particles of electrodeposited zinc hydroxochloride. The loss of water vapor and HCl upon heat treatment apparently leads to consolidation of the individual $Zn_5(OH)_8Cl_2$ layers to give nanocrystals of ZnO and the formation of nanometric cavities between these nanocrystals.

The absorption spectra of the $Zn_5(OH)_8Cl_2$ films (Fig. 2a, curve 1) show a structureless band, which is a halo resulting from light scattering. After heating the films and their conversion into ZnO, a band with a washed-out edge appears at 370-390 nm (3.18-3.35 eV) and pronounced maxima at 360-365 nm (3.40-3.45 eV) on the background of the light scattering

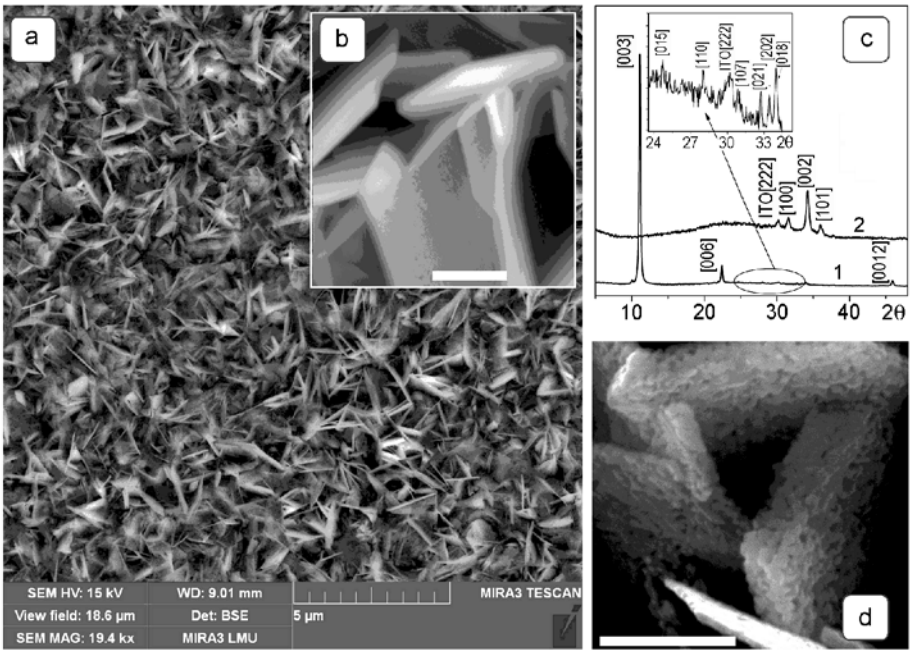

Fig. 1. a) Electron microphotography of an ITO/$Zn_5(OH)_8Cl_2$, b) an enlarged fragment of microphotograph a, scale 500 nm, c) diffraction patterns of electrodeposited films prior (1) and after roasting at 400 °C (2) (the indices of the faces related to the reflections are given in brackets; the assignment was carried out using the international diffraction data base (ICDD No. 07-0155 for $Zn_5(OH)_8Cl_2$, ICDD No. 036-1451 for ZnO, ICDD No. 01-089-4596 for ITO); an enlarged fragment of pattern 1 is given in the insert, d) fragment of an electron microphotograph of the ITO/ZnO film, scale 500 nm.

halo. In order to determine the forbidden band gap E_g of ZnO, we used the Tautz formula for the absorption coefficient of a semiconductor (SC) [13]:

$$\alpha = A\frac{(h\nu - E_g)^n}{h\nu} \tag{1}$$

where α is the SC absorption coefficient, A is a constant, and $h\nu$ is the light quantum energy, while the power n depends on the nature of the transition and is 1/2 in the case of ZnO [1, 4-8, 13]. The derivative of Eq. (1)

$$\frac{d(\ln(\alpha h\nu))}{d(h\nu)} = \frac{n}{h\nu - E_g} \tag{2}$$

has a discontinuity at $h\nu = E_g$ (see Fig. 2a, insert), which permits us to determine the value of E_g with high accuracy. The value of E_g thereby found for zinc oxide was 3.30 eV, which corresponds to the forbidden band of massive ZnO, for which values have been given in the range 3.20-3.37 eV depending on the type of crystal structure [1, 4, 13]. The presence of a band with maximum at E = 3.40-3.45 eV, which is shifted by 0.10-0.15 eV toward higher energies relative to E_g of massive ZnO, indicates the presence of particles existing in the spatial restraint mode of photogenerated electron–hole pairs and similar in diameter to the exciton Bohr diameter for zinc oxide (5 nm) [8, 13]. The evaluations carried out using a calibration [8, 13] relating the electron transition energy in ZnO nanocrystals with their diameter show that this band indeed belongs to particles with diameter

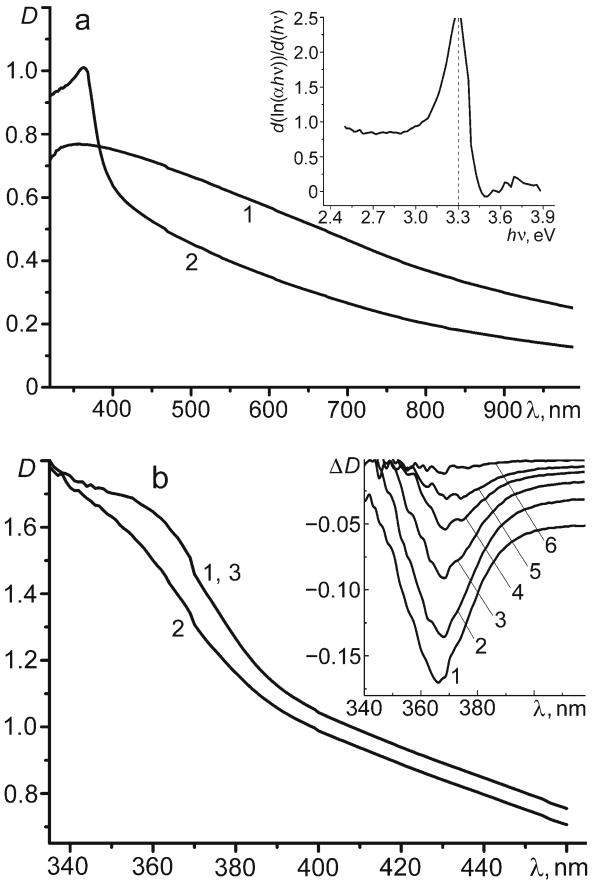

Fig. 2. a) Absorption spectra of films ITO/$Zn_5(OH)_8Cl_2$ (1) and ITO/ZnO (2) (the insert gives anamorphosis 2 as a plot for $d(\ln(\alpha h\nu))/d(h\nu) - h\nu$; the dashed line gives the discontinuity point of the curve), b) absorption spectrum of the ITO/ZnO film in ethanol bubbled with argon prior to irradiation (1), after 10 min irradiation at λ = 310-390 nm (2) and after the introduction of air into the irradiated solution and maintenance for 15 min in the dark (3) (the insert gives differential absorption spectra of the ITO/ZnO film (relative to the absorption spectrum of the nonirradiated film) immediately after cessation of irradiation and the introduction of air (1) and after maintaining the film in the air in the dark for 15 s (2), 5 (3), 7 (4), 9 (5) and 14 min (6)).

of about 5 nm. The relatively small spectral width of this band (~40 nm) indicates that the particles, which give rise to this band, have a narrow size distribution.

On first glance, we might propose that particles with diameter 20-40 nm comprising the ZnO microplates in the film, in turn, consist of smaller "building blocks" of ZnO particles with 5 nm diameter. However, this proposal is contradicted by the XPA data discussed above, indicating the mean coherent X-ray scattering region for ITO/ZnO films is 20 nm. The mass fraction of ZnO particles with 5 nm diameter in these samples is clearly small. Located at sites of contact of larger zinc oxide crystallites, the smaller particles may act as a unique cement imparting mechanical strength to the planar microparticles. Furthermore, as shown by the data considered below, despite the low content of ZnO nanoparticles, they apparently have a

decisive effect on the photochemical properties of the electrodeposited films, in particular, their capacity to undergo photoinduced charging and the nature of their photocatalytic properties.

The irradiation of ITO/ZnO films immersed in absolute ethanol saturated with argon at 310-390 nm leads to a hypsochromic shift of the edge of the ZnO absorption (Fig. 2b, curves 1 and 2). This shift displays saturation behavior by reaching 0.20-0.22 eV during the initial 5-10 min of film irradiation and then remaining unchanged upon further exposure of the films as well as upon its subsequent maintenance for several weeks in the dark in the absence of electron acceptors, in particular, atmospheric oxygen. The absorption band of the ITO/ZnO film gradually returns to its original position after the inlet of air (compare curves 1 and 3 in Fig. 2b). These features of the photoinduced spectral shift, specifically, its saturation, reversibility, and sensitivity to the presence of an electron acceptor, permit us to relate it to the dynamic Burstein–Moss effect reported for colloidal ZnO solutions, i.e., an increase in the electronic transition energy (optical width of the forbidden band) due to occupation of some of the states at the bottom of the conductance band of the ZnO nanoparticles by photogenerated electrons [5-8, 13]. This behavior is favored by the presence of an excess of electron donor (ethanol) in the system, which captures the photogenerated holes of the ZnO valence band and prevents the recombination of these holes with electrons of the conductance band.

In light of the nature of the Burstein–Moss effect displayed and the magnitude of the photoinduced shift, these ZnO films are extremely similar to previously studied colloidal solutions of zinc oxide containing 4-6-nm particles [5-7]. On the other hand, in contrast to the colloidal systems, in which the photoinduced shift disappears several seconds after the inlet of air into the solutions due to the rapid draw-off of excess electrons to O_2 molecules, the return of the absorption band edge for the ZnO films observed here to its initial position requires hundreds of seconds of maintenance in contact with an air-saturated solvent (see the insert in Fig. 2b). Furthermore, the photoinduced shift in the case of electrodeposited ZnO films reaches saturation several times more rapidly and is retained upon subsequent maintenance in the dark in the absence of air much longer than in the case of colloidal ZnO nanoparticles. This behavior is also apparently related to the much higher rate of discharge of these nanoparticles in reaction with the solvent.

The magnitude of the spectral shift due to the Burstein–Moss effect is known to depend on the excess charge density n_e to the 3/2 power [13, 14]. Since n_e, in turn, is inversely proportional to the particle volume or to the cube of its radius, it may be readily shown that upon going from colloidal ZnO particles with diameter ~5 nm, for which the photoinduced shift is 0.18-0.22 eV [6], to ZnO particles with diameter 20-40 nm, which predominantly comprise the electrodeposited zinc oxide films, the shift should be diminished by a factor of $\sim 10^3$. On the other hand, the observed Burstein shift is the same for the colloidal nanoparticles and the ZnO films. Hence, zinc oxide crystals with diameter 20-40 nm, which predominate in the electrodeposited ZnO films, cannot participate in their photoinduced charging. Apparently, the fraction of small 5-nm particles, whose presence in the films is indicated by a maximum in their absorption spectra, play the major role in the capacity of ZnO films to accumulate charge.

The dynamics of the change in intensity of the bands in the differential absorption spectra of irradiated ZnO films (Fig. 2b, insert) indicates that the discharge processes in the electrodeposited ZnO films occurs over hundreds of seconds, which is one or two orders of magnitude slower than with the participation of colloidal ZnO nanoparticles [5-7]. The unusually low rate of the dark discharge of such nanoparticles is mostly likely a consequence of their difficult accessibility for oxygen molecules. Such a situation might well obtain when, as proposed above, small ZnO particles are located between the larger crystallites, which shield them from contact with the solvent. We note that a photoinduced Burstein–Moss effect has been observed for the first time in zinc oxide film materials using continuous UV irradiation.

It would be natural to assume that the pronounced capacity of electrodeposited ZnO films to accumulate and retain excess charge can significantly affect the nature of the photochemical and photocatalytic processes involving such films, especially those involving overvoltage or multiple electrons [5, 7]. A typical example of such a process may be seen in the photoreduction of $NaAuCl_4$ by ethanol [7, 13, 15]. In previous work [7], we have shown that this reaction in the presence of colloidal ZnO particles with diameter 5-6 nm becomes photocatalytic and leads to the formation of metallic gold nanocrystals with diameter 20-30 nm. A feature of this process is the rather long induction period, after which the reaction proceeds more rapidly and with self-catalysis up to complete conversion of the gold(III) salt. As we have shown in previous work [7], the low photoreduction rate at the onset is related to the need to convert ZnO nanoparticles upon the action of light into a charged state, in which the three-electron reduction of Au(III) is considerably facilitated. The appearance of gold nanoparticles in the system

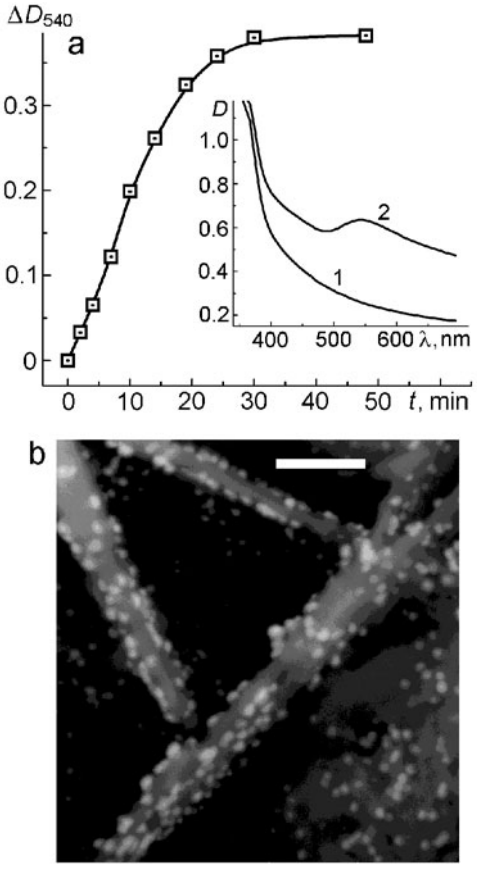

Fig. 3. a) Kinetic curve corresponding to the increase in the optical density of an ITO/ZnO film immersed in argon-saturated ethanol containing $1.0 \cdot 10^{-4}$ mol/L $NaAuCl_4$ due to irradiation at λ = 310-390 nm (the insert gives the absorption spectra of the ITO/ZnO film at λ = 540 nm prior to (1) and after exposure for 40 min (2)), b) scanning electron microphotograph of the ITO/ZnO/Au film obtained at 40 min exposure, scale 200 nm.

capable of efficiently accepting photoelectrons from ZnO particles and accumulating significant greater charge leads to an increase in the reaction rate and conversion to self-catalysis.

Photocatalytic properties in the reduction of Au(III) by ethanol are also characteristic for electrodeposited zinc oxide films. Ultraviolet irradiation of ZnO films immersed in ethanolic solutions of $NaAuCl_4$, both saturated with argon and containing oxygen, leads to the appearance of plasmon resonance absorption with maximum at 540-560 nm characteristic for metallic gold [15] in the absorption spectra (Fig. 3a, insert). The SEM data showed that gold is deposited on the surface of the ZnO microplates as particles with diameter 20-40 nm (Fig. 3b).

A feature of the photocatalytic reduction of Au(III) on the surface of electrodeposited ZnO films, which distinguishes this reaction from its analog involving colloidal zinc oxide particles [7], is the lack of an induction period and very poorly defined self-catalysis characteristics. In light of features discussed above for the photoinduced charging of electrodeposited ZnO films, such a photoprocess may be attributed to the pronounced capacity of these films to accumulate excess charge. As noted in our previous work [7], the conversion of the photocatalytic reduction of Au(III) in zinc oxide colloids to a self-catalysis

mode is related to the appearance of gold particles in the system and ZnO-Au heterostructures with greater capacity to undergo charging and three-electron reduction of Au(III) than the initial ZnO nanoparticles. On the other hand, in the case of electrodeposited ZnO films displaying enhanced capacity to undergo photoinduced charging, the appearance of an additional photoelectron accumulator, namely, gold nanoparticles, apparently has hardly any effect on the dynamics of Au(III) reduction such that this process displays only weak self-catalysis.

Thus, nanocrystalline zinc oxide films on the ITO surface were obtained by electrodeposition. These films are composed of ZnO microplates with diameter 0.5-2.0 μm and thickness 50-300 nm, which, in turn, consist of nanocrystals with diameter 20-40 nm. Analysis of the spectral data indicated the presence of particle fractions with diameter of about 5 nm in the zinc oxide microplates. These fractions impart the capacity to undergo photoinduced charging to the ZnO films. Discharge of the films proceeds at a rate slower by one or two orders of magnitude than in the case of colloidal ZnO solutions containing particles with diameter 4-6 nm. The pronounced capacity of zinc oxide films to accumulate photoelectrons significantly affects the kinetics of the photocatalytic reduction of $NaAuCl_4$ by ethanol involving these films.

This work was carried out with the support of the State Basic Research Fund of Ukraine (Project No. F41.3/005).

REFERENCES

1. F. Xu and L. Sun, *Energy Environ. Sci.*, **4**, No. 3, 818-841 (2011).
2. Z. Chen, Y. Tang, L. Zhang, et al., *Electrochim. Acta*, **51**, No. 26, 5870-5875 (2006).
3. Y. Y. Xi, Y. F. Hsu, A. B. Djurišić, et al., *J. Electrochem. Soc.*, **155**, No. 9, 595-598 (2008).
4. Q. Zhang, C. S. Dandeneau, X. Zhou, et al., *Adv. Mater.*, **21**, No. 41, 4087-4108 (2009).
5. A. L. Stroyuk, V. V. Shvalagin, I. E. Kotenko, et al., *Teor. Éksp. Khim.*, **46**, No. 4, 212-217 (2010). [*Theor. Exp. Chem.*, **46**, No. 4, 218-224 (2010) (English translation).]
6. V. V. Shvalagin, A. L. Stroyuk, and S. Ya. Kuchmii, *J. Nanopart. Res.*, **9**, No. 3, 427-440 (2007).
7. O. L. Stroyuk, V. V. Shvalagin, I. E. Kotenko, et al., *Khim., Fiz. Tekhnol. Poverkhn.*, **1**, No. 2, 119-127 (2010).
8. M. Haase, H. Weller, and A. Henglein, *J. Phys. Chem.*, **92**, No. 8, 482-487 (1988).
9. L. Xu, Q. Chen, and D. Xu, *J. Phys. Chem. C*, **111**, No. 31, 11560-11565 (2007).
10. M. Moriya, K. Yoshikawa, W. Sakamoto, et al., *Inorg. Chem.*, **48**, No. 17, 8544-8549 (2009).
11. T. Hongo, T. Iemura, S. Satokawa, et al., *Appl. Clay Sci.*, **48**, No. 3, 455-459 (2010).
12. B. P. Pichon, A. Mezy, J.-C. Tedenac, et al., *New J. Chem.*, **33**, No. 11, 2350-2354 (2009).
13. O. L. Stroyuk, S. Ya. Kuchmiy, A. I. Kryukov, and V. D. Pokhodenko, *Semiconductor Catalysis and Photocatalysis on the Nanoscale*, Nova Sci. Publ., Inc., New York (2010).
14. C.-Y. Liu and A. J. Bard, *J. Phys. Chem.*, **93**, No. 8, 3232-3237 (1989).
15. S. K. Ghosh and T. Pal, *Chem. Rev.*, **107**, No. 11, 4797-4862 (2007).